A Eulerian-Lagrangian approach for the CFD analysis of airborne disease transmission in a car cabin

A Eulerian-Lagrangian approach for the CFD analysis of airborne disease transmission in a car cabin

G. Grossi[1], F. Arpino[1], G. Buonanno[1], G. Cortellessa[1], L. Moretti[1], H. Nagano[2], L. Stabile[1]

[1]Department of Civil and Mechanical Engineering, University of Cassino and Southern Lazio, Cassino, FR, Italy

[2]Department of Mechanical Systems Engineering, Tokyo City University, 1-28-1 Tamazutsumi, Setagaya-ku, Tokyo, 158-8557, Japan

giorgio.grossi@unicas.it

Abstract. In indoor environments such as private cars, taxis and public transport, social distance cannot always be applied and virus concentrations can reach high levels. In this paper, a Eulerian-Lagrangian approach is adopted for the transient simulation of aerosol airborne dispersion in a passenger car cabin. The numerical tool, validated by PIV analysis, is applied to study three different scenarios during the respiratory activity. The car ventilation system and the position of the passengers affect the mass of inhaled aerosol and consequently the quality of the passenger compartment air.

1. Introduction

The risk of virus infection can be reduced by adopting different strategies such as social distancing and the adoption of masks in order to avoid virus diffusion particularly in indoor environments [1,2]. The thermodynamics phenomena related to breathing, coughing, speaking and sneezing are complicated therefore it is impossible to measure virus transport and diffusion in indoor environments [3].

In the last century, the large droplet route has been wrongly considered to be the primary route for most respiratory infections [4,5], and the associated social distancing of 1-2 m has been adopted in all the country of the world. The respect of a social distance represents a good measure in open spaces but it cannot be adopted in small indoor environments like car cabins where the occupants are in a close range and, during a car trip, the virus concentrations can reach crucial levels [6].

In fact, droplets of different sizes, coming from different areas of the respiratory tract, go through an atomization process by the passage of a high-speed air stream. Wells et.al. [7] studied the phenomenon of droplet evaporation during breathing from the mouth of a subject and the particle diameters reduction during the air injection. Further investigations were performed by Papineni et al. [8] adopting an optical particle detection system. In particular, the authors found that most of the particles present micrometres diameters (<100 μm) and, after an evaporation process, can reach the susceptible suspended in air (airborne particles) [9]. As said before, in open spaces there is a low risk of contracting infections because virus concentrations are very low [10]. On the contrary, in indoor environments such as public transport, hospital rooms, schools, on which a lot of infected people are in close contact even when social distance is applied, the infection risk is very high. Suggestions to reduce the increasing in virus concentrations in indoor consists in the improvement of the ventilation system, the surfaces disinfection,

the reduction of the number of occupants, etc. However, more effective forecasting and analysis tools are desirable to allow a more detailed understanding about measures to be adopted inside restricted environments like passenger cars. Computational Fluid Dynamics (CFD) allow to obtain detailed information about transport and diffusion of aerosol also for the case of private transport such as for a car cabin. This technique get detailed spatial fluid flow distributions and aerosol transmission by solving a 3D mixed convection model in transient conditions [11,12] and it also allows to assess the ventilation conditions of aerosol transmission by solving a 3D mixed convection model in transient conditions. A lot of research was conducted to improve the airflow distribution in passenger cabins.
PIV (Particle Image Velocimetry) analysis were conducted by Yang et al. [13,14] to investigate airflow distribution and turbulence intensity in selected car cabin sections.
You et al. [15] investigated the suitable turbulence model to simulate air distribution in aircraft cabins with gaspers turned on. They showed that the SST k–ω model was more accurate than the RNG k–ε model for predicting the airflow distribution in an aircraft cabin. Mathai et al. [16] analysed how the windows opening and closing can affect the thermo-hygrometric comfort and the aerosol spread between the passengers discovering that addressing the airflow from the ventilation system away from passengers reduces the risk of transmission.
The numerical studies available in the scientific literature present same limitations which can be highlighted such as a simplified numerical modelling of the breathing phenomena in isothermal conditions and the absence of buoyancy effects. Moreover, such models do not distinguish the droplets variation in diameter during the respiratory activity and the effective mass flow rate injected during breathing by an emitter subject. In other cases, a velocity boundary condition is not set on the mouth of the receiver to properly simulate the breathing phenomenon, also considering the aerosol inhalation.
In the present paper, the OpenFOAM open-source software is adopted to simulate the transient non-isothermal airborne aerosol dispersion in a passenger car cabin. The model is based on a Eulerian-Lagrangian approach: mass, momentum and energy conservation equations are solved for the description of the fluid flow distribution within the computational domain, while Newton's equation is adopted for the diffusion and transport of particles. The numerical model was validated by comparing the numerical results with PIV measurements, performed by one of the authors of the paper and then applied to study the aerosol transport, spatial distribution and inhalation during respiratory activity, from one specific person (contagious subject) to another passenger (receiver subject) inside a car cabin for different ventilation scenarios.

2. CFD numerical model

CFD simulations were performed by the OpenFOAM code which can solve the mass, momentum and energy conservation equations for 3D transient and turbulent compressible fluid flow. The numerical tool gives information about the pressure, temperature and velocity contours in the investigated computational domain. Turbulence was modelled using the Unsteady Reynolds Averaged Navier Stokes (URANS) approach, solving the Shear Stress Transport (SST) k–ω model since it is well suited for simulating induced jet flows in closed environments, as proven by previous studies of You et al. [15] and Ullrich et al. [17]. Further information about the solved Partial Differential Equations (PDEs) can be found in [18].

The aerosol transport and diffusion were obtained by adopting a Lagrangian Particle Tracking (LPT) approach, based on a dispersed dilute two-phase flow. This model can be adopted when droplets are distant one from each other and their volume is lower than 10^{-3}. In this way, the mass momentum and energy equations are solved for the air flow (continuous phase) and the Newton's equation of motion is solved for each droplet (discrete phase). LPT equations are obtained by solving Equation 1 and Equation 2.

$$m_d \frac{d\boldsymbol{u}_d}{dt} = \boldsymbol{F}_D + \boldsymbol{F}_g \quad (1)$$

$$\frac{d\boldsymbol{x}_d}{dt} = \boldsymbol{u}_d \tag{2}$$

where $m_d\ (kg)$ is the mass of the droplet; $\boldsymbol{u}_d\left(\frac{m}{s}\right)$ represents the droplet velocity; $t\ (s)$ is the time; $\boldsymbol{F}_D\ (N)$ and $\boldsymbol{F}_g(N)$ are, respectively, the drag and gravity forces acting on the droplet; $\boldsymbol{x}_d\ (m)$ represents the trajectory of the droplet. The drag force is given by Crowe [19]:

$$\boldsymbol{F}_D = m_d \frac{18}{\rho_d \cdot d_d^2} C_D \frac{Re_d(\boldsymbol{u} - \boldsymbol{u}_d)}{24} \tag{3}$$

In Equation 3, $\rho_d\left(\frac{kg}{m^3}\right)$, $d_d(m)$ and Re_d represent, respectively, the density, diameter and Reynolds number of the droplet; $\boldsymbol{u}\left(\frac{m}{s}\right)$ is the air velocity. The droplet density was considered constant and equal to 1200 kg·m^{-3}. The Re_d was calculated as:

$$Re_d = \frac{\rho(|\boldsymbol{u} - \boldsymbol{u}_d|)d_d}{\mu} \tag{4}$$

where $\rho\left(\frac{kg}{m^3}\right)$ is the air density.
The drag coefficient, C_D, in Equation 3 is evaluated as a function of the droplet Reynolds number:

$$C_D = \begin{cases} \dfrac{24}{Re_d} & \text{if } Re_d < 1 \\ \dfrac{24}{Re_d}\left(1 + 0.15 \cdot Re_d^{0.687}\right) & \text{if } 1 \le Re_d \le 1000 \\ 0.44 & \text{if } Re_d > 1000 \end{cases} \tag{5}$$

Droplet collisions are considered to be elastic and the equations of motion for the droplets are solved assuming a one-way coupling between the continuum phase and the discrete phase: the flow field affects the droplet motion whereas the effect of the particles on the airflow is negligible.

3. The three investigated scenarios

The mathematical-numerical model described in Section 2 was applied to the analysis of droplets spread in a passenger car cabin during a 15-min travel, from one contagious subject (i.e. the driver in our analysis) to a susceptible receiver (i.e. another passenger). Three different scenarios were analysed: a) air supplied from front seat vents and susceptible sitting in the back-right seat (Figure 1a); b) air supplied from the windshield defroster vent and susceptible sitting in the back-right seat (Figure 1b); c) air supplied from the windshield defroster vent and susceptible sitting in the front seat (Figure 1c).
The numerical model validation was performed by a scaled-down glass model by adopting PIV analysis (Figure 2) but to investigate a real scenario it was increased in size by a scale factor equal to 1.7 as indicated in the study of Chang in [20] by reducing the seats inclination. A typical car volumetric flow rate equal to 238 m^3/h was imposed as boundary condition in inlet from the ventilation system and the volume of the scaled-up car cabin model is equivalent to that of a typical real car [17]. Inlet boundary condition for air temperature was set to 293 K and the heat exchange with the environment was not modelled. The mouths of the passengers were modelled as a circle with a 2 cm radius and a temperature of 308.15 K was adopted as boundary conditions for the resolution of the energy equation conservation equation.
An averaged fixed velocity value of 0.61 m/s was employed at the mouths of the emitter and the receiver as mean values of sinusoidal breathing during exhalation and inhalation reported by Abkarian et al. [21]. This choice allows to reach a quasi-steady state condition: once the quasi-steady state condition is

achieved, the flow field is frozen and is used to transport the particles injected by the emitter over time while breathing.
Droplets were assumed as liquid spheres whose dimensions, distribution and injection time were adopted from existing literature [3,22]. Evaporation phenomenon occurs soon after the injection [9], so in the present study the number and volume distribution of droplet after evaporation were considered.
The simulations were carried out assuming the subjects to be mouth-breather.

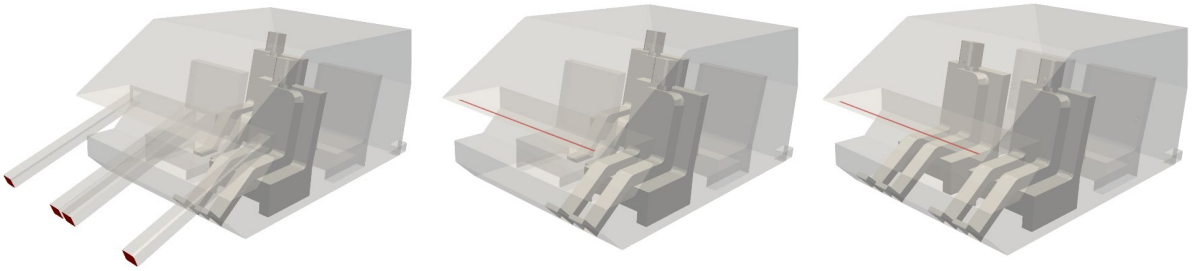

(a) front seat air vents supply mode – susceptible in the back-right seat

(b) windshield defroster air vent supply mode – susceptible in the back-right seat

(c) windshield defroster air vent supply mode – susceptible in the front seat

Figure 1 – The three analysed scenarios where the inlet sections are highlighted in red.

4. Validation of the numerical tool by PIV analysis

The flow field description within the passenger compartment was validated with the Particle Image Velocimetry (PIV) data which one of the authors obtained in a previous experimental campaign [14], for the scaled-down car cabin model shown in Figure 2a. Experimental analysis were performed along the longitudinal plane passing through the centre of the air vent in front of the driver seat (within the x-y plane at z=0.3945 m, as highlighted in Figure 4). The fluid flow is injected inside the cabin through four openings located on the dashboard, at a total flow rate equal to 100 m^3/h; in the experimental setup a rectangular duct is connected to each of the supply openings, causing a flow velocity profile to develop at the outlet section of the air vents (at the entry of the passenger compartment; for more details refer to [14]).
In the 3D model employed for numerical model validation, shown in Figure 2b, such ducts were considered to reproduce the velocity distribution at the inlet of the cabin and accurately replicate the experimental conditions. The adopted mesh was obtained by the tool *snappyHexMesh* and was determined on the basis of a proper grid sensitivity analysis. Four computational grids were realized and information about the grids parameters are illustrated in Table 1.

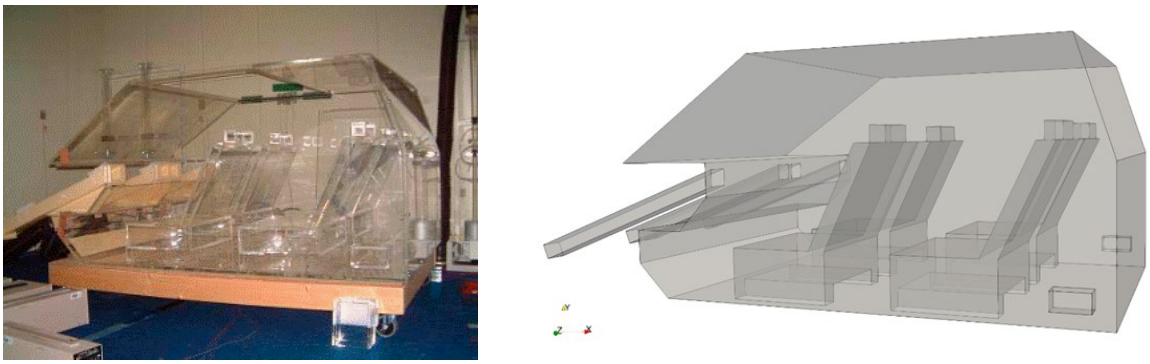

(a) scale car model for PIV measurements [14]

(b) computational domain

Figure 2 – Scaled glass model adopted for PIV analysis (a) and computational domain (b).

Table 1 – Computational grid information

Mesh #	Number of Cells	Skewness max	Non orthogonality max
1	355,534	1.44	50
2	743,232	3.45	50
3	1,559,007	2.19	50
4	2,905,119	3.78	50

The percent deviation amongst the velocity fields obtained with Mesh 3 and Mesh 4 is less than 5%, hence Mesh 3 has been used in the upcoming analysis. In Figure 3, a x-y slice of Mesh 3 for z=0.3945 m (measuring plane) is shown.

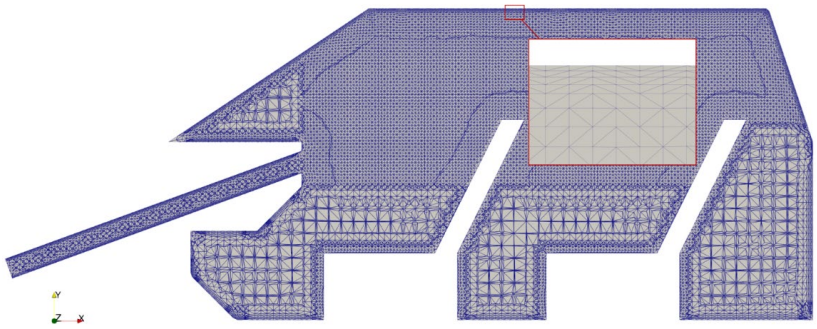

Figure 3 – Computational grid employed (Mesh 3, 1559007 cells) for velocity field validation.

The computational grid was refined near solid surfaces to properly capture the boundary layer; moreover, a refinement box was created in the upper zone of the car cabin to have a finer mesh in the area of most interest for the comparison with the experimental velocity profiles, without requiring unreasonable computational efforts. The minimum, maximum and average y^+ values obtained using Mesh 3 are 0.129, 41.484 and 5.472 respectively. PIV and CFD data were compared in terms of velocity profiles obtained in a a selected x-y plane at z=0.3945 m (see Figure 4), in four different sections: x=0.45 m, x=0.65 m, x=0.85 m and x=1.05 m.

On the whole, it was found that the airflow patterns predicted with CFD simulations are in a good agreement with the experimental results provided by Ozeki et al. [14], even when getting away from the inlet sections. Therefore, the mathematical-numerical model adopted in the present study well describes the flow field within the car cabin.

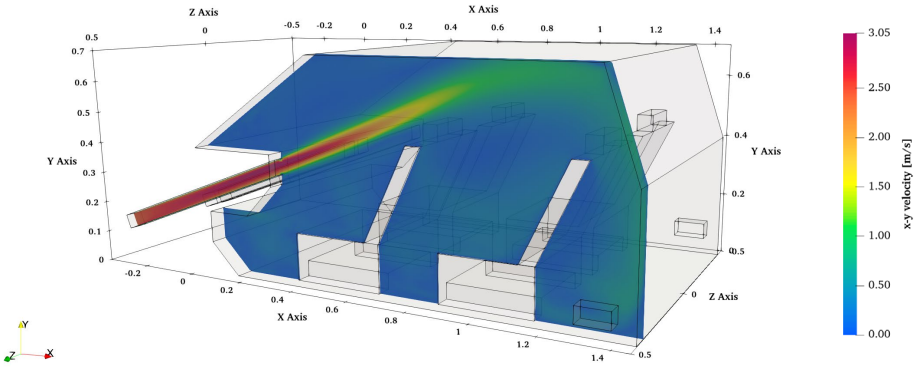

Figure 4 – Velocity contours for a slice located at z=0.3945 m.

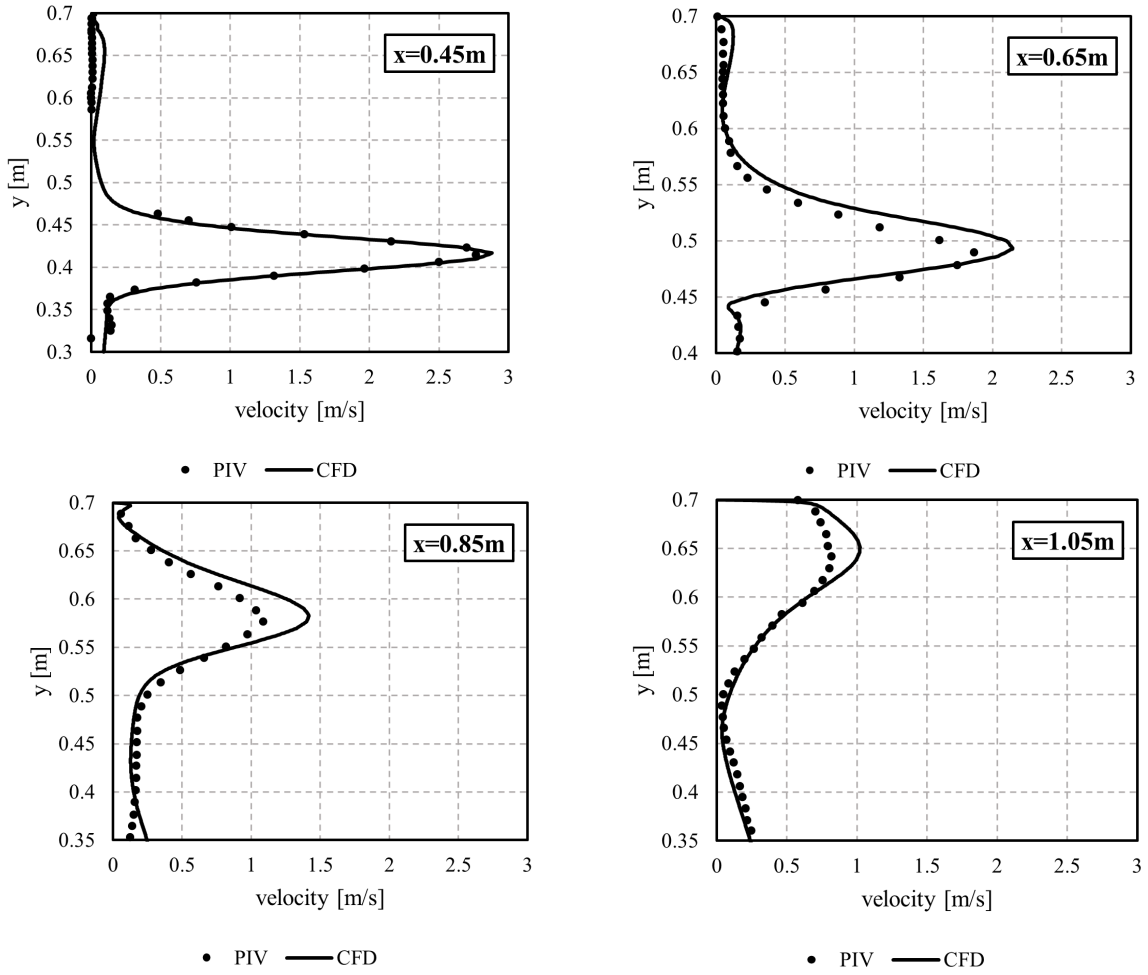

Figure 5 – Experimental and numerical velocity profiles comparison within a selected x-y plane at z=0.3945 m obtained in four different sections: x=0.45 m, x=0.65 m, x=0.85 m and x=1.05 m.

5. Results obtained by CFD analysis

In Figure 6 the particles position in the car cabin after 15 minutes, for the scenarios outlined in Section 3, is showed. Adopting the front seat vents (Figure 6a) the passengers do not receive particles because a recirculation area is formed above the dashboard and airborne droplets are not able to reach the subject position. On the contrary, turning on the windshield defroster (Figure 6b and Figure 6c), there is a quite uniform distribution of particles within the cabin. The passenger located in the back-right seat (Figure 6b), inhales about 20 particles (corresponding to a mass of $1.56 \cdot 10^{-15}$ kg), instead when he is placed in the front seat (Figure 6c), he receive about 15 particles (corresponding to a mass of $5.42 \cdot 10^{-16}$ kg). Although after 15 minutes the number of inhaled particles is not significant, by increasing the time spent in the car cabin the mass of inhaled aerosol could reach critical values. Therefore, a parametric analysis, varying the flowrate at the inlet and the time spent in the car, will be performed in later studies to assess how these aspects influence the motion, and thus the spread of droplets in the passenger compartment.

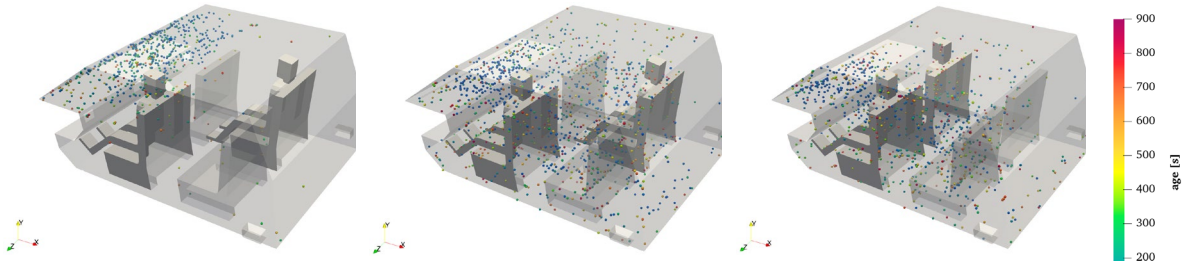

(a) front seat air vents supply mode - susceptible in the back-right seat

(b) windshield defroster air vent supply mode – susceptible in the back-right seat

(c) windshield defroster air vent supply mode – susceptible in the front seat

Figure 6 – Evolution of particles after 15 minutes.

6. Conclusions

In the present paper, the authors realized an innovative transient non-isothermal numerical model by using the open-source software OpenFOAM, able to simulate the transient airborne dispersion of aerosol in a passenger car cabin. The model is based on a Eulerian-Lagrangian approach: mass, momentum and energy conservation equations are solved for the description of the fluid flow distribution within the computational domain, while Newton's equation is adopted for diffusion and transport of particles. The numerical model was validated by comparing the numerical results with PIV measurements, performed by one of the authors of the paper. The validated numerical tool was applied to study the aerosol transport, spatial distribution and inhalation, during respiratory activity, from one specific person (contagious subject) to another passenger (receiver subject) inside a car cabin for different ventilation scenarios. The car ventilation system and the position of the passengers affect the mass of inhaled aerosol and consequently the quality of the passenger compartment air.

References

[1] Qian H, Miao T, Liu L, Zheng X, Luo D and Li Y 2021 Indoor transmission of SARS-CoV-2 *Indoor Air* **31** 639–45
[2] Blocken B, Malizia F, van Druenen T and Marchal T 2020 Towards aerodynamically equivalent COVID-19 1.5 m social distancing for walking and running
[3] Morawska L, Johnson G R, Ristovski Z D, Hargreaves M, Mengersen K, Corbett S, Chao C Y H, Li Y and Katoshevski D 2009 Size distribution and sites of origin of droplets expelled from the human respiratory tract during expiratory activities *Journal of Aerosol Science* **40** 256–69
[4] Chapin C V 1912 *The sources and modes of infection* (New York: J. Wiley & sons)
[5] Flügge C 1897 Ueber Luftinfection *Zeitschr. f. Hygiene.* **25** 179–224
[6] Buonanno G, Stabile L and Morawska L 2020 Estimation of airborne viral emission: Quanta emission rate of SARS-CoV-2 for infection risk assessment *Environment International* **141** 105794
[7] Wells W F 1934 ON AIR-BORNE INFECTION* *American Journal of Epidemiology* **20** 611–8
[8] Papineni R S and Rosenthal F S 1997 The Size Distribution of Droplets in the Exhaled Breath of Healthy Human Subjects *Journal of Aerosol Medicine* **10** 105–16
[9] Balachandar S, Zaleski S, Soldati A, Ahmadi G and Bourouiba L 2020 Host-to-host airborne transmission as a multiphase flow problem for science-based social distance guidelines *International Journal of Multiphase Flow* **132** 103439
[10] Coccia M 2020 Factors determining the diffusion of COVID-19 and suggested strategy to prevent future accelerated viral infectivity similar to COVID *Science of The Total Environment* **729** 138474
[11] Lewis R W, Nithiarasu P and Seetharamu K N 2004 *Fundamentals of the finite element method for heat and fluid flow* (Hoboken, NJ: Wiley)

[12] Scungio M, Arpino F, Cortellessa G and Buonanno G 2015 Detached eddy simulation of turbulent flow in isolated street canyons of different aspect ratios *Atmospheric Pollution Research* **6** 351–64
[13] Yang J H, Kato S and Nagano H 2009 Measurement of airflow of air-conditioning in a car with PIV *J Vis* **12** 119–30
[14] Ozeki Y, Yang J-H, Nagano H, Kato S, Nomura E, Inoue M and Kobayashi S 2008 Ventilation Characteristics of Modeled Compact Car Part 1 Airflow Velocity Measurement with PIV *SAE Int. J. Passeng. Cars – Mech. Syst.* **1** 631–9
[15] You R, Chen J, Shi Z, Liu W, Lin C-H, Wei D and Chen Q 2016 Experimental and numerical study of airflow distribution in an aircraft cabin mock-up with a gasper on *Journal of Building Performance Simulation* **9** 555–66
[16] Mathai V, Das A, Bailey J A and Breuer K 2021 Airflows inside passenger cars and implications for airborne disease transmission *Sci. Adv.* **7** eabe0166
[17] Ullrich S, Buder R, Boughanmi N, Friebe C and Wagner C 2020 Numerical Study of the Airflow Distribution in a Passenger Car Cabin Validated with PIV *New Results in Numerical and Experimental Fluid Mechanics XII* Notes on Numerical Fluid Mechanics and Multidisciplinary Design vol 142, ed A Dillmann, G Heller, E Krämer, C Wagner, C Tropea and S Jakirlić (Cham: Springer International Publishing) pp 457–67
[18] Versteeg H K and Malalasekera W 2007 *An introduction to computational fluid dynamics: the finite volume method* (Harlow, England ; New York: Pearson Education Ltd)
[19] Crowe C T 2012 *Multiphase flows with droplets and particles* (Boca Raton: CRC Press)
[20] Chang T-B, Sheu J-J, Huang J-W, Lin Y-S and Chang C-C 2018 Development of a CFD model for simulating vehicle cabin indoor air quality *Transportation Research Part D: Transport and Environment* **62** 433–40
[21] Abkarian M, Mendez S, Xue N, Yang F and Stone H A 2020 Speech can produce jet-like transport relevant to asymptomatic spreading of virus *Proc Natl Acad Sci USA* **117** 25237–45
[22] Johnson G R, Morawska L, Ristovski Z D, Hargreaves M, Mengersen K, Chao C Y H, Wan M P, Li Y, Xie X, Katoshevski D and Corbett S 2011 Modality of human expired aerosol size distributions *Journal of Aerosol Science* **42** 839–51